SUPPLEMENTARY INFORMATION

Green Microalgae *Scenedesmus obliquus* Utilization for the Adsorptive Removal of Nonsteroidal Anti-Inflammatory Drugs (NSAIDs) from Water Samples

Andreia Silva [1], Ricardo N. Coimbra [2], Carla Escapa [3], Sónia A. Figueiredo [1], Olga M. Freitas [1] and Marta Otero [2,4,*]

[1] REQUIMTE/LAQV, Instituto Superior de Engenharia Do Porto, Politécnico Do Porto, Rua Dr. António Bernardino de Almeida 431, Porto, 4200-072, Portugal; andreia.silva@graq.isep.ipp.pt (A.S.); saf@isep.ipp.pt (S.A.F.); omf@isep.ipp.pt (O.M.F.)

[2] Department of Environment and Planning, University of Aveiro, Campus Universitário de Santiago, Aveiro, 3810-193, Portugal; ricardo.coimbra@ua.pt (R.N.C.)

[3] Department of Applied Chemistry and Physics, Institute of Environment, Natural Resources and Biodiversity (IMARENABIO), Universidad de León, León, 24071, Spain; carla.escapa@unileon.es (C.E.)

[4] Centre for Environmental and Marine Studies (CESAM), University of Aveiro, Campus Universitário de Santiago, Aveiro, 3810-193, Portugal

* Correspondence: marta.otero@ua.pt; +351 234247094 /ext: 25010 (M.O.)

Contents

Figure S1 depicts the species distribution diagram as a function of pH for salicylic acid and ibuprofen (respectively adapted from [1] and [2]).The pH value impacts the charge of the species in solution [3,4]. In the case of salicylic acid, diprotic species (neutral) are dominant (about 90%) at pH values below 2, monoprotic species (negative) are dominant at pH values between 4 and 13 and completely dissociated species (negative) are dominant (about 70%) at pH values above 13 [2] (see Figure S1(a)) The carboxylic group of ibuprofen is not charged at low solution pH (equal or below to *pK*a). However, as the solution pH increases from 3 to 7, the carboxylic group begins to dissociate and almost all ibuprofen molecules are negatively charged when the solution pH is above 7 [1,5] (see Figure S1(b))

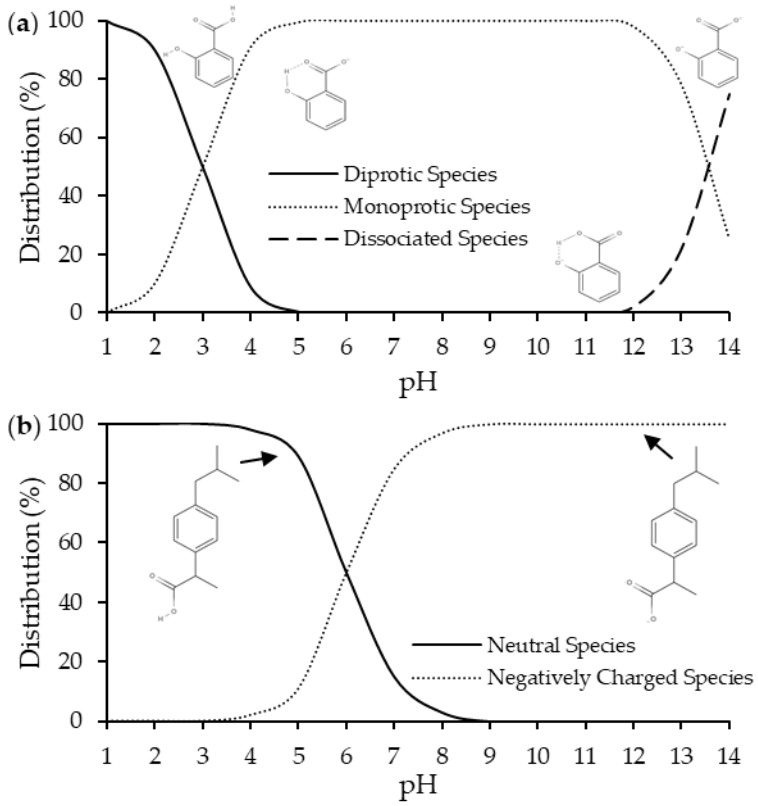

Figure S1. Species distribution diagram of (**a**) salicylic acid and (**b**) ibuprofen as a function of pH (adapted from: [1] and [2], respectively).

Simultaneous thermal analysis (STA) allows identifying mass losses and thermal transitions occurred during the decomposition of *Scenedesmus obliquus* biomass before and after pharmaceuticals biosorption through the interpretation of TG/DTG curves over time are shown in Figure S2.

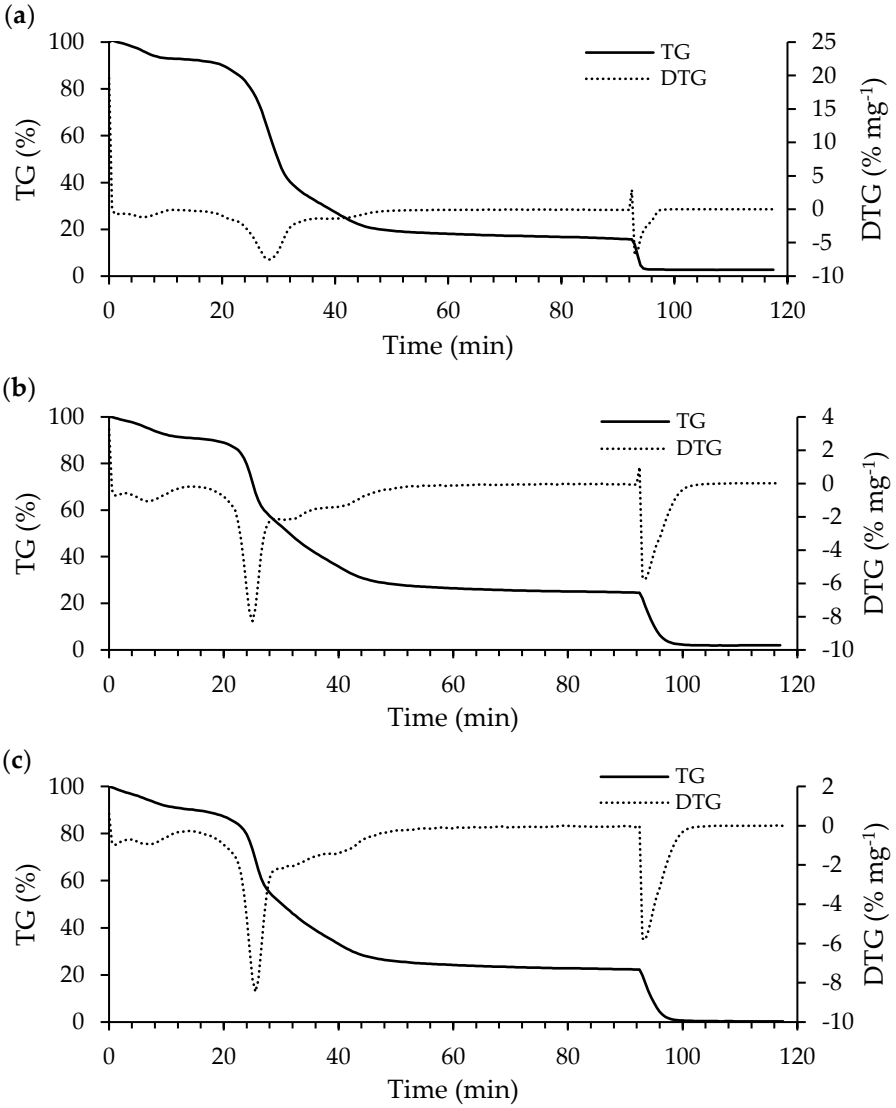

Figure S2. Thermogravimetry (TG) together with derivative thermogravimetry (DTG) curves over time of *Scenedesmus obliquus* biomass before biosorption (**a**); and after salicylic acid (**b**) or ibuprofen (**c**) biosorption.

Differential scanning calorimetry (DSC) together with derivate differential scanning calorimetry (DDSC) curves give complementary information to TG/DTG curves, namely in terms of energy consumption or liberation. Therefore, DSC/DDSC provide more precise information about the occurring transformations on microalgae biomass. The onset temperature (T_{onset}) and the endset temperature (T_{enset}) are, respectively, the temperatures that define the start and the end of a thermal event in DSC/DDSC curves, used to determine the enthalpy (ΔH) by peak integration. The maximum temperature ($T_{DSC,max}$) is the temperature of maximum energy released during a thermal event.

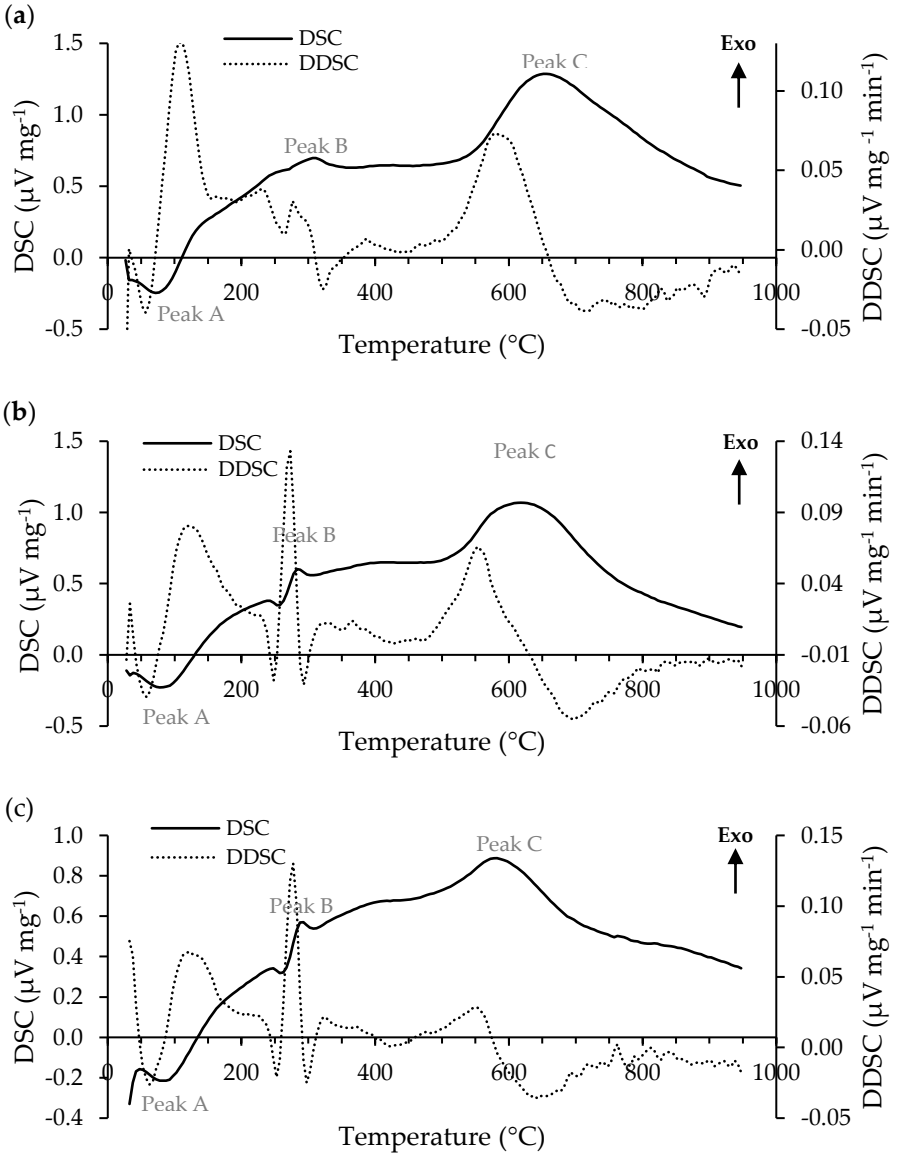

Figure S3. Differential scanning calorimetry (DSC) together with derivate differential scanning calorimetry (DDSC) curves of *Scenedesmus obliquus* biomass before biosorption (**a**); and after salicylic acid or ibuprofen (**b**) biosorption.

Table S1. Physicochemical properties of the commercial activated carbon used as reference (Pulsorb WP260), as provided by the producer (Chemviron Carbon, Feluy, Belgium).

Specifications	
Specific Surface Area, SBET (m^2 g^{-1})	1050
Iodine number (mg g^{-1})	1020
Mean particle diameter (μm)	30
Density, loose packing (kg m^{-3})	250

With respect to other materials used for the biosorption of salicylic acid or ibuprofen from water, Table 2 depicts some recently published Q_{max} and makes evident that the here determined values for *Scenedesmus obliquus* biomass are within the range of values in the literature.

Table S2. Maximum salicylic acid or ibuprofen biosorption capacities (Q_{max} (mg g^{-1})) of different materials in the literature.

Biosorption of Salicylic acid			**Biosorption of Ibuprofen**		
Material	**Q_{max} (mg g^{-1})**	**Reference**	**Material**	**Q_{max} (mg g^{-1})**	**Reference**
Sterile Malmo soil (Alfisols)	18	[6]	Functionalized bean husks	32	[7]
Sterile Drummer soil (Mollisols)	12	[6]	Modified *Scenedesmus obliquus* biomass	42	[8]
Sterile Jefferson (Ultisols)	57	[6]	Knotweed leaves	38	[9]
Scenedesmus obliquus biomass	63	This work	*Phaeodactylum tricornutum* biomass	4	[10]
			Scenedesmus obliquus biomass	12	This work

Table S3. Fitted equilibrium parameters on the adsorption of salicylic acid and ibuprofen onto *Scenedesmus* biomass at the different temperatures considered in this work.

		Salicylic acid			Ibuprofen		
		15°C	**25°C**	**35°C**	**15°C**	**25°C**	**35°C**
Freundlich	K_F (mg g^{-1} (mg L^{-1})$^{-1/n}$)	13 ± 3	10 ± 2	5.8 ± 1.2	4.1 ± 0.6	3.4 ± 0.3	2.7 ± 0.4
	n	2.6 ± 0.4	2.51 ± 0.07	2.0 ± 0.2	3.7 ± 0.5	3.7 ± 0.3	3.8 ± 0.6
	r^2	**0.914**	**0.945**	**0.958**	**0.923**	**0.970**	**0.970**
	$S_{y.x}$	6.57	4.57	3.62	12.4	0.87	0.56
Langmuir	Q_{max} (mg g^{-1})	67 ± 3	63 ± 2	62 ± 3	14.1 ± 0.3	11.9 ± 0.3	9.6 ± 0.3
	K_L (L mg^{-1})	0.10 ± 0.02	0.070 ± 0.005	0.066 ± 0.004	0.12 ± 0.01	0.11 ± 0.01	0.087 ± 0.011
	r^2	**0.985**	**0.996**	**0.994**	**0.994**	**0.994**	**0.991**
	$S_{y.x}$	2.76	1.23	1.31	0.37	0.32	0.31

Table S4. Band assignments of Fourier transform infrared (FT-IR) spectra of *Scenedesmus obliquus* biomass before and after salicylic acid and ibuprofen biosorption.

Band	Wavenumber (cm^{-1})			Band Assignments [1]	References
	S. obliquus	*S. obliquus* after biosorption of			
		Salicylic acid	Ibuprofen		
A	**3408**	**3405**	3423	ν(O-H) (associated) to water molecules or hydroxyl radicals of polysaccharides ν(N-H) (associated) to proteins (amide A)	[11–14] [11,12,14]
B	2924	2924	2924	$\nu_{as}(CH_2)$ of lipids	[11–16]
C	2853	2853	-------	$\nu(CH_2)$ of lipids	[11–13,15]
D	1655	1655	1655	ν(C=O) of amides I band associated with proteins	[11–15,17]
E	1545	1541	1541	δ(N-H) of amides II band and δ(C-N) of proteins	[11–17]
F	-------	1458	1458	$\delta_{as}(CH_2)$ of lipids $\delta_{as}(CH_2)$ and $\delta_{as}(CH_3)$ of proteins	[11–14] [11,12,14,15,17]
G	1384	1383	1383	$\delta_s(N(CH_3)_3)$ of lipids $\delta_s(CH_2)$ and $\delta_s(CH_3)$ of proteins, and ν_s(C-O) of carboxylic groups	[11,13,14,16] [11,13–17]
H	1246	1244	1241	ν_{as}(>P=O) of phosphodiester backbone from nucleic acids and phospholipids	[11–15,17]
I	1153	1154	1154	ν_{as}(C-O) of starch and complex sugar ring modes ν(C-O-C) of polysaccharides (from carbohydrates) ν(Si-O) of silicate frustules	[11,13,14] [13–15,17] [15]
J	1078	1079	1079	ν_{as}(C-O) of starch and complex sugar ring modes ν_{as}(>P=O) of phosphodiester backbone from nucleic acids ν(C-O-C) of polysaccharides (from carbohydrates) ν(Si-O) of silicate frustules	[1–14,16] [11–14] [13–17] [15,17]
K	1025	1025	1026	ν_{as}(C-O) of starch and complex sugar ring modes ν_{as}(>P=O) of phosphodiester backbone from nucleic acids ν(C-O-C) of polysaccharides (from carbohydrates) ν(Si-O) of silicate frustules	[11,13,14] [11,13,14] [12–15,17] [15]

[1] ν - stretching; ν_s - symmetric stretching; ν_{as} - asymmetric stretching; δ - deformation; δ_s - symmetric deformation; δ_{as} - asymmetric deformation.

Table S5. Characteristic parameters of differential scanning calorimetry (DSC) together with derivate differential scanning calorimetry (DDSC) curves determined for *Scenedesmus obliquus* biomass before and after salicylic acid and ibuprofen biosorption.

Peak	Parameters [1]	*S. obliquus*	*S. obliquus* after biosorption of	
			Salicylic acid	Ibuprofen
A	T_{onset} (°C)	26.9	28.0	72.9
	$T_{DSC,max}$ (°C)	71.9	77.7	84.2
	T_{endset} (°C)	130.2	151.2	146.3
	ΔH (μV mg^{-1})	−131	−101	−17
B	T_{onset} (°C)	223.8	262.8	277.1
	$T_{DSC,max}$ (°C)	309.5	284.4	290.0
	T_{endset} (°C)	343.6	297.9	303.4
	ΔH (μV mg^{-1})	47	17	10
C	T_{onset} (°C)	540.5	517.9	498.1
	$T_{DSC,max}$ (°C)	651.0	618.4	579.4
	T_{endset} (°C)	866.5	758.3	766.4
	ΔH (μV mg^{-1})	3246	1315	592

[1] T_{onset} - onset temperature for energy release and peak integration; $T_{DSC,max}$ - temperature of maximum energy release during process; T_{enset} - endset temperature for energy release during process; ΔH - enthalpy determined by integration of the peak in the corresponding DSC curve.

References

1. Singh, R.; Hankins, N. *Emerging Membrane Technology for Sustainable Water Treatment*, 1st ed.; Elsevier Science: Oxford, UK 2016.
2. Bernal, V.; *et al.* Thermodynamic study of the interactions of salicylic acid and granular activated carbon in solution at different pHs. *Adsorption Science & Technology*, **2017**, 36(3-4), 833-850, doi:10.1177/0263617417730463.
3. Davis, T.A.;*et al.*, A review of the biochemistry of heavy metal biosorption by brown algae. *Water Research*, **2003**, 37(18), 4311-4330, doi:10.1016/S0043-1354(03)00293-8.
4. Ozer, A.;*et al.* Biosorption of Acid Blue 290 (AB 290) and Acid Blue 324 (AB 324) dyes on *Spirogyra rhizopus. J Hazard Mater*, **2006**, 135(1-3), 355-64, doi:10.1016/j.jhazmat.2005.11.080.
5. Oh, S.; *et al.* Effects of pH, dissolved organic matter, and salinity on ibuprofen sorption on sediment. *Environ Sci Pollut Res Int*, **2016**, 23(22), 22882-22889, doi:10.1007/s11356-016-7503-6.
6. Jagadamma, S.; *et al.* Selective sorption of dissolved organic carbon compounds by temperate soils. *PLoS One*, **2012**, 7(11), e50434, doi:10.1371/journal.pone.0050434.
7. Bello, O.S.; *et al.* Biosorption of ibuprofen using functionalized bean husks. S*ustainable Chemistry and Pharmacy*, **2019**, 13, doi:10.1016/j.scp.2019.100151.
8. Ali, M.E.M.; *et al.* Removal of pharmaceutical pollutants from synthetic wastewater using chemically modified biomass of green alga *Scenedesmus obliquus. Ecotoxicol Environ Saf,* **2018**, 151, 144-152, doi:10.1016/j.ecoenv.2018.01.012.
9. Mucha, M.; Mucha, M. Ibuprofen and acetylsalicylic acid biosorption on the leaves of the knotweed Fallopia x bohemica. *New Journal of Chemistry*, **2017**, 41(16), 7953-7959, doi:10.1039/C7NJ01658A
10. Santaeufemia, S.; Torres, E.; Abalde, J. Biosorption of ibuprofen from aqueous solution using living and dead biomass of the microalga *Phaeodactylum tricornutum. Journal of Applied Phycology*, **2017**, 30(1), 471-482, doi:10.1007/s10811-017-1273-5.
11. Sigee, D.C.; *et al.* Fourier-transform infrared spectroscopy of Pediastrum duplex: characterization of a micro-population isolated from a eutrophic lake. *European Journal of Phycology*, **2002**, 37(1), 19-26, doi:10.1017/S0967026201003444.
12. Ponnuswamy, I.; *et al.* Isolation and Characterization of Green Microalgae for Carbon Sequestration, Waste Water Treatment and Bio-fuel Production. *International Journal of Bio-Science and Bio-Technology*, **2013**, 5, 17-26.
13. Grace, C.E.E.; *et al.* Biomolecular transitions and lipid accumulation in green microalgae monitored by FTIR and Raman analysis. *Spectrochim Acta A Mol Biomol Spectrosc*, **2020**, 224, 117382, doi:10.1016/j.saa.2019.117382.
14. Dilek, D. Fourier transform infrared (FTIR) spectroscopy for identification of *Chlorella vulgaris* Beijerinck 1890 and *Scenedesmus obliquus* (Turpin) Kützing 1833. *African Journal of Biotechnology,* **2012**, 11(16), doi:10.5897/AJB11.1863.
15. Giordano, M.; *et al.* Fourier Transform Infrared Spectroscopy as a Novel Tool to Investigate Changes in Intracellular Macromolecular Pools in the Marine Microalga *Chaetoceros Muellerii (Bacillariophyceae). Journal of Phycology*, **2002**, 37(2), 271-279, doi:10.1046/j.1529-8817.2001.037002271.x.
16. Wen, Y.; *et al.* Enantioselective ecotoxicity of the herbicide dichlorprop and complexes formed with chitosan in two fresh water green algae. *J Environ Monit*, **2011**, 13(4), 879-85, doi:10.1039/c0em00593b.
17. Stehfest, K.; *et al.* The application of micro-FTIR spectroscopy to analyze nutrient stress-related changes in biomass composition of phytoplankton algae. *Plant Physiol Biochem*, **2005**, 43(7), 717-26, doi:10.1016/j.plaphy.2005.07.001.